FERMILAB-CONF-08-198-TD

DARK CURRENT MODEL FOR ILC MAIN LINAC*

N. Solyak#, G. Romanov, N.V. Mokhov, FNAL, Batavia, IL 60510,
Y. Eidelman, BINP, Novosibirsk, Russia.
Wai-Ming Tam, Indiana University, Bloomington, IN

Abstract

In the ILC Main Linac, the dark current electrons, generated in SRF cavity can be accelerated to hundreds of MeV before being kicked out by quadrupoles and thus will originate electromagnetic cascade showers in the surrounding materials. Some of the shower secondaries can return back into vacuum and be re-accelerated again. The preliminary results of simulation of the dark current generation in ILC cavity, its dynamics in linac are discussing in this paper.

INTRODUCTION

High gradient superconducting RF may produce electrons emitted from the cavity surface that may be captured in accelerating regime. Since dark current particles have broad angular, space and phase distribution, particles will be lost somewhere in downstream cavities causing undesirable effects, like heat and RF loading of the cavity and production of avalanches of secondary electrons. This process may limit performance of the ILC cryomodule. It is important to simulate dark current and understand dynamics in the ILC linac. In this paper we present very preliminary results. The first part of study is simulation of the dark current production in one ILC cavity at gradient 30 MV/m. The second part is developing model of the ILC linac in the MARS15 code [1] which can simulate both propagation of the dark current in linac lattice and interaction of the particles with the surrounding media – walls of the cavity, helium and walls of titanium vessel. Interaction with media is not started yet and we are planning to do this in this year with the goal a) reproduce and cross-check results of dark current simulations done for the XFEL project [2] and b) study dark current deposition for the ILC main linac and bunch compressor.

PARTICLE TRACKING IN 9-CELL CAVITY

Since the task is to figure out how the dark current electrons are captured into acceleration and what this accelerated dark current beam looks like at the exit of the cavity, 9-cell TESLA cavity has been replaced by a MWS model without HOM couplers, and a perfect field distribution was considered (see Fig.1). To calculate the particle trajectories, a tracking code has been written in VBA for use in Microwave Studio environment. The tracking code uses smooth approximated fields and solid models created by MWS. The code solves the relativistic equations of particle motion in RF fields combined with uniform static magnetic field. Buneman-Boris method is used to solve the equations of motion.

In RF accelerating cavities electric field is variable in time and has highly non-uniform surface distribution. As a result field emission can not occur everywhere and at all times. As a function of time (or rf phase) the emitted current is approximately Gaussian, with rms width $\sqrt{\beta E / 6.53 \cdot 10^9 \phi_e^{1.5}}$ [3]. For copper at surface field of 85-130 MV/m and enhancement factor of 30 it varies from 11° to 14°. For niobium cavity a surface field of 60 MV/m is expected at accelerating gradient of 30 MV/m. Assuming working function for niobium 4.3 eV and $\beta = 30$ we have rms width of appropriate phases ≈10°. So, the interval of initial phases of 70°-110° should be considered, assuming $E = E_0 \cdot \sin(\omega t + \phi)$.

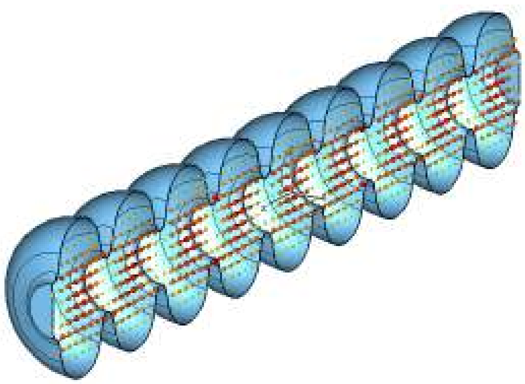

Figure 1: MWS model of 9-cell TESLA cavity.

The field emission takes place on the surfaces with highest surface electric field. For TESLA type cavity maximum surface field is on the irises. The extensive particle tracking have been performed at accelerating gradient of 30 MV/m to define more precisely the emission sites and the interval of phases at which the emitted electrons are captured into acceleration. It turned out that the area of "successful" emission is rather small as it seen in Fig. 2. The appropriate emission area is 2-4 mm wide ring on both sides of iris. The tracking also shown that the relevant interval of phases shrinks as well from 70°-110° to 88°-110°, because the electrons emitted at phases <88° just cannot go out from cell.

After the emission areas and appropriate for emission phases were found, the final tracking has been performed. The goal of tracking was to determine high field emission current parameters at the end of the cavity as a sum of emission currents from all irises. The particles were emitted one by one from high surface field area on each of 9 irises at fixed accelerating field phase of 95° and accelerating gradient of 30 MV/m. The cavity has axial

*Work supported by Fermi Research Alliance, LLC, under contract No. DE-AC02-07CH11359 with the U.S. Department of Energy.
#solyak@fnal.gov

symmetry and symmetry relatively to its center, so it is sufficient to consider emission in one plane (Y-plane) and from one side of irises (right side as shown in Fig. 2). Then all particles from all irises that have been accelerated and reached the cavity's exit are analyzed. Of course, the flight time for particles from different irises is different, but after 8-9 RF periods there is a steady ensemble of particles from all irises at any moment.

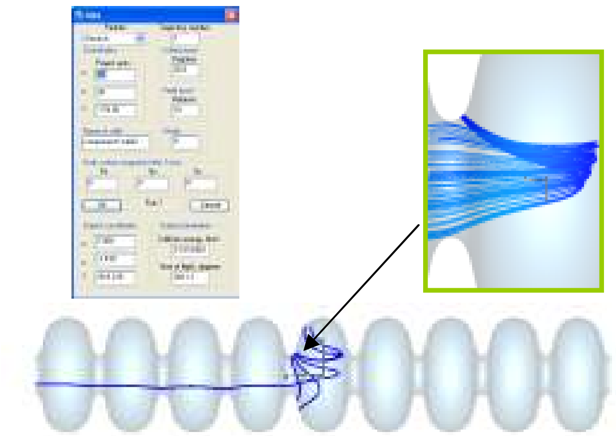

Figure 2: Electrons emitted from narrow area only can get through aperture and be accelerated. GUI of tracking code is also shown.

For each iris 60-80 particle trajectories were simulated to get reasonable density of particles at the cavity exit and saved in data files. Then an additional program written in Mathematica analyzed the data and saved the results for further use in MARS. Figs. 3 and 4 show the plots of some data sets created by this program.

For different initial phases of emission in the interval of 88-110°, the beam parameters are very similar. But density of emitted current changes very rapidly according to the Fowler-Nordheim theory of field emission. As a result, the normalized beam density at the exit of the cavity changes significantly. The integral (sum of currents from all irises emitted in interval of 88-110°) current density over phase space is shown in Fig. 5.

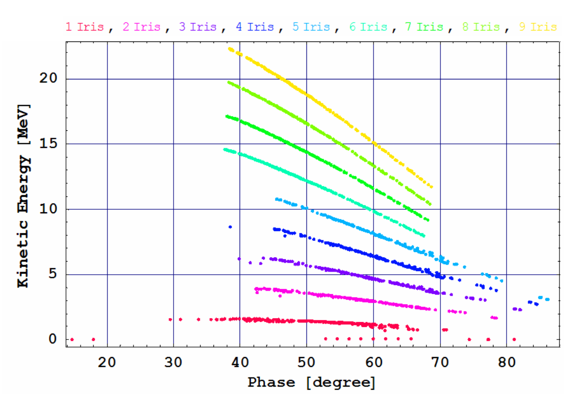

Figure 3: Kinetic energy of electrons *vs*. RF phase at the cavity exit. Points corresponding to different irises have different colors.

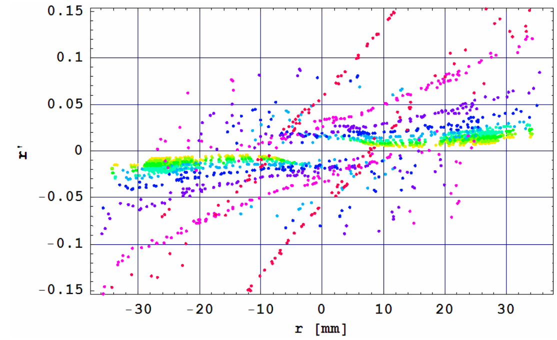

Figure 4: Transverse emittances at the cavity exit.

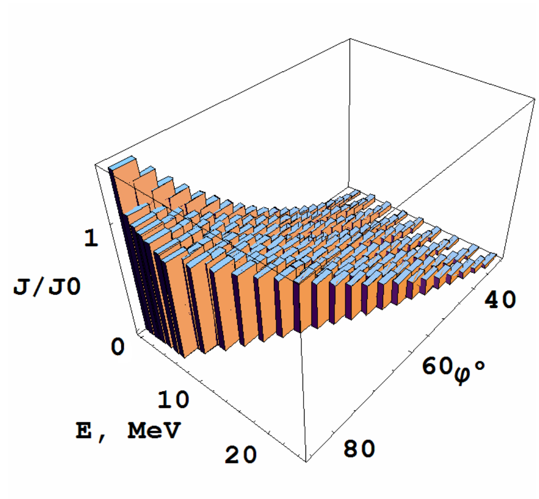

Figure 5: The integral of current density over phase space.

DARK CURRENT PROPAGATING IN ILC LINAC

For beam dynamics simulation of the dark current in a regular accelerating structure of the ILC the MARS15 Monte-Carlo code was used. Its structure is flexible and easily allows to include special user-developed sub-programs, which can accommodate needs for the specific task. MARS is dedicated and effective code for modeling particle interactions with media, but not quite adequate for simulation of accelerating beam physics. That's why along with developing special user routines, the tracking part of MARS15 was improved to simulate beam propagation in cavities.

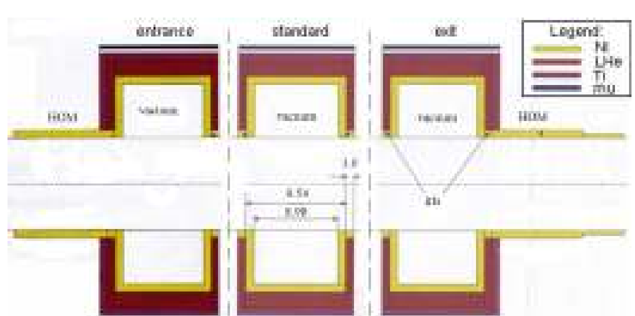

Figure 6: Simplified geometry of the 9-cell ILC cavity in MARS. Here only three cells are shown: input, middle (regular) and output.

For the purpose of this study, a simple pill-box shape was used instead of the elliptical one (Fig. 6). In the first step, niobium was replaced with an artificial, so-called “black hole”, material which guarantees that any particle touching this material will disappear without producing secondary particles. Realistic modeling of showers generated in niobium, helium media and titanium vessel, is not done yet and is a subject of further studies. Some of secondary electrons can come back to the cavity and contribute to the dark current dynamics [2].

ILC quadrupoles are the key element for cleaning dark current. They focus high-energy main beam, but over-focus low-energy dark current particles. Each quadrupole is located in the middle of a cryomodule replacing one of the cavities. The ILC lattice used in simulation has a 75°/60° phase advance per FODO cell with one quad per 3 cryomodules (9-8-9 cavities in each). For modeling behaviour of dark current in the vicinity of quadrupoles, we investigated build-up of the dark current in preceding cavities. Fig. 7 shows the trajectories of ~60 particles (out of 2469 generated in cavities), that reached focusing quad with the gradient G=2.34T/m corresponding to low energy part of the main Linac (15GeV).

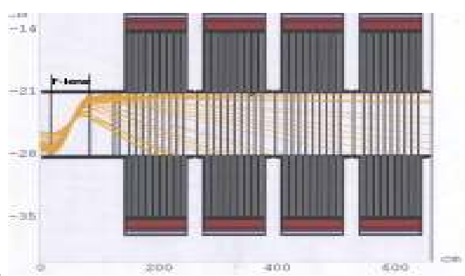

Figure 7: Trajectories of the survived dark current particles in focusing quad followed by 4 cavities.

One can see that the major part of particles is lost after the focusing quad at the walls of downstream cavities. Simulation shows that only ~25% of particles generated in a cavity reach next cavity and this portion dramatically falls down in next cavities, as shown in Fig. 8.

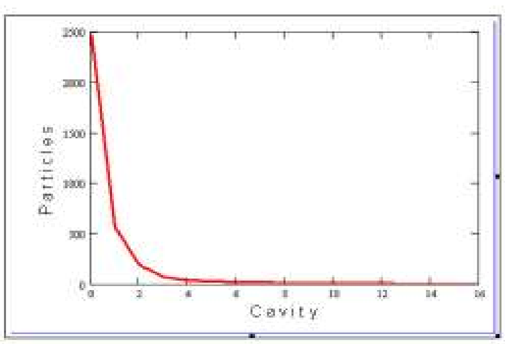

Figure 8: Number of dark current particles that reached upstream cavities. Only particles generated in cavity #0 are taken into account. In last four cavities 7 particles survived and captured in acceleration.

Fig. 9 shows radial, angular and phase distributions of the particles generated in cavity #0 at the entrance of 17 downstream cavities. This information is used for generation of dark current distribution at the entrance of each quadrupole by summing all particles generated in each cavity in between of two quadrupoles (this is standard accelerating module for linac). It simplifies dark current simulations, allowing tracking onlythose particles that survived after preceding quadrupole and then add at the entrance of the next quadrupole a new particle ensemble generated in all cavities of this module.

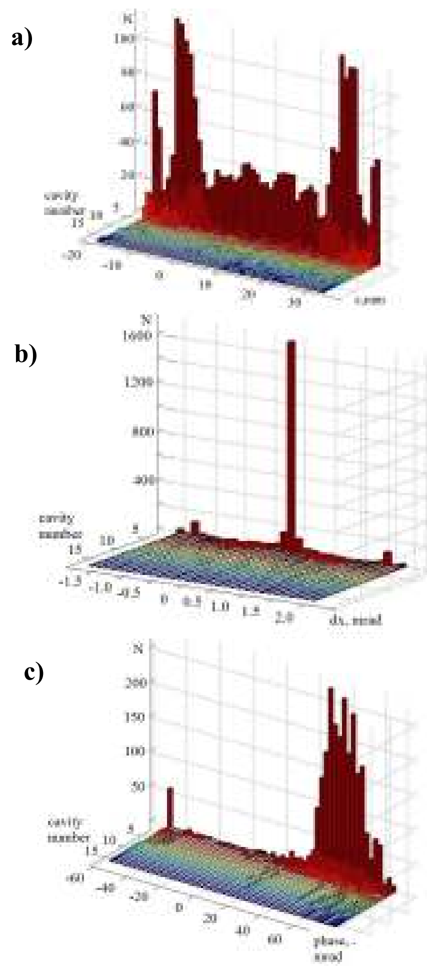

Figure 9: Distribution of particles generated in cavity#0 at the entrance of each upstream cavity: a) ***x***-radial distribution; b) ***dx*** - angular distribution; c) phase distribution.

REFERENCES

[1] N.V. Mokhov, http://www-ap.fnal.gov/MARS/

[2] V.Balandin et all, Studies of Electromagnetic Cascade Showers Development in the TESLA Main Linac Initiated by Electron Field Emission in RF Cavities, DESY, Hamburg, TESLA Report 2003-10

[3] K.Bane et al, “Dark current and their effect on the primary beam in an X-band linac”, Physical Review Special Topic – Accelerators and Beams, **8,** 064401 (2005).